

Roughening and smoothing behavior of Al/Zr multilayers grown on flat and saw-tooth substrates

D.L. Voronov,* E.H. Anderson, R. Cambie, E.M. Gullikson, F. Salmassi, T. Warwick, V.V. Yashchuk, and H.A. Padmore

Lawrence Berkeley National Laboratory, 1 Cyclotron Road, Berkeley, CA 94720, USA

*email: dlvoronov@lbl.gov

ABSTRACT

Diffraction gratings with high efficiency and high groove density are required for EUV and soft x-ray spectroscopy techniques (such as Resonant Inelastic X-ray Scattering, RIXS) designed for state-of-the-art spectral resolution and throughput. A multilayer coated blazed grating (MBG) fabricated by deposition of a multilayer on a saw-tooth substrate could address these challenges. In order to obtain high diffraction efficiency one should provide perfect triangular grooves on a substrate and perfect replication of the groove profile during the multilayer deposition. However, multilayers tend to smooth out the corrugated surface of the substrates, resulting in the main limiting factor for efficiency of ultra-dense MBGs. Understanding of the growth of multilayers on saw-tooth substrates is a key for further grating improvement. In this work we investigate growth behavior of Al/Zr multilayers on saw-tooth substrates with a groove density of 10,000 lines/mm. We apply existing growth models to describe an evolution of Power Spectral Density functions of a grating surface during the multilayer deposition, and identify a main smoothing mechanism. We found that growth of flat multilayers is well modeled with surface diffusion caused by surface curvature as a main relaxation mechanism, while growth of the multilayer on saw-tooth substrates obeys different kinetics. Limitations of the linear approach and possible model improvements by accounting for an additional component of the surface diffusion flux, caused by a gradient of adatom concentration on a corrugated surface are discussed.

Key words: diffraction grating, multilayer, wet anisotropic etch, EUV, soft x-rays, surface morphology, roughening, relaxation, Power Spectral Density.

1. INTRODUCTION

Recent progress in fabrication of high quality saw-tooth gratings with anisotropic wet etch of Si [1] opens promising opportunities for development of ultra-high resolution gratings for EUV and soft x-ray applications [2]. In order to obtain high diffraction efficiency a grating should be coated with a multilayer reflector. Performance of such a multilayer coated blazed grating (MBG) is defined by both quality of the substrate and perfection of the multilayer stack. Previous investigation of the structure of a Mo/Si MBG showed that multilayer do not replicate the substrate profile but trend to smooth it out [3]. For Al/Zr MLG this effect is much more pronounced and results in a sine-like shape of the grooves [4]. The distortions of the saw-tooth grooves have a negative impact on the blazing ability of the grating and seem to be a main limiting factor for diffraction efficiency of MBGs. While deposition of the MLs on flat substrates is a well established process, growth of MLs on saw-tooth substrates has not been extensively studied. Understanding of the processes which are behind the smoothing is necessary for optimization of a deposition process and grating design, and crucial for further progress in MBG performance.

There are several models for evolution of the surface of a coating during its growth or erosion [5]. The models are based on a continuum equation which in the simplest linear case is;

$$\frac{\partial h(\mathbf{r},t)}{\partial t} = -\sum_n v_n \nabla^n h(\mathbf{r},t) + \eta(\mathbf{r},t) \quad (1)$$

where $h(\mathbf{r},t)$ is a surface height, \mathbf{r} is a radius vector, t is a time of the deposition (or a coating thickness provided the deposition rate is constant), v_n is a relaxation parameter, $\eta(\mathbf{r},t)$ is a white noise caused by fluctuations of the incoming atomic flux. The second term in the right part of the equation (1) describes surface roughening caused by stochastic

nature of a deposition or sputtering process, and the second one represents relaxation of a surface with one or several mass transport mechanisms. The main relaxation mechanisms were identified as viscous flow ($n = 1$), evaporation and condensation ($n = 2$), volume diffusion ($n = 3$), and surface diffusion ($n = 4$) [6]. Later $n = 2$ was attributed to sputter erosion [7], and downhill current smoothing mechanism [8] which is basically a pure ballistic effect.

Equation (1) can be solved in a reciprocal space. This leads to a Power Spectral Density (PSD) function for a surface of a film growing on ideally smooth and flat substrate as

$$PSD(f, d) = \Omega \frac{1 - \exp(-2d \sum v_n f^n)}{\sum v_n f^n} \quad (2)$$

where f is a spatial frequency, d is a film thickness, Ω is an atomic volume, and v_n is a relaxation parameter which related to a relaxation length, l , via

$$l^{n-1} = v_n \quad (3)$$

PSD evolution of a coating growing on an initially rough substrate ($PSD_{sub} \neq 0$) is described by

$$PSD_{tot} = PSD_{film} + a^2 PSD_{sub} \quad (4)$$

where a is a frequency dependent replication factor

$$a = \exp(-d v_n f^n) \quad (5)$$

This model was successfully applied for simulation of PSDs for many x-ray multilayers deposited on flat substrates [9,10]. Later the linear model was slightly modified in order to take into account a material contraction due to formation of a silicide interlayers at the Mo/Si interfaces, and successfully used for simulation of smoothing of relatively big artificially introduced defects on a substrate during deposition of ion-beam-sputtered Mo/Si multilayers [11].

In this work we will apply the model for description of the growth the Al/Zr multilayers and discuss the model limitations and suggest some improvements of the model regarding the multilayer growth.

2. EXPERIMENT

Al/Zr multilayers consisting of 20 bilayers with the bi-layer thickness of 10 nm were deposited by dc-magnetron sputtering on silicon wafers and saw-tooth substrates. The semiconductor prime quality silicon wafers with a regular chemical-mechanical surface finish were used as flat substrates for the multilayer deposition. The same silicon wafers were used for fabrication of silicon blazed gratings with a period of 100 nm and a blaze angle of 6 degrees [4] with anisotropic wet etch of silicon [12]. The gratings were used as saw-tooth substrates for the multilayer deposition. Both the saw-tooth and the flat substrates were deposited with the Al/Zr multilayers simultaneously under the same sputtering conditions.

The surface of the substrates was characterized before and after the deposition with a Veeco Dimension-3100 Atomic Force Microscope (AFM).

3. RESULTS

A typical AFM image of the surface of silicon wafers used in this work as substrates for Al/Zr multilayer deposition is shown in Fig. 1a. The wafers were processed by a vendor with regular chemical-mechanical surface finish, which provides high surface smoothness in the high spatial frequency range. Though some residual scratches are observed on the AFM image, the roughness does not exceed 0.1 nm rms as measured over a $1 \times 1 \mu m^2$ area. A two-dimensional isotropic PSD function of the surface, shown in Fig. 2 with grey squares, reveals a typical fractal-like power law $PSD \sim 1/f^n$.

Deposition of Al/Zr multilayers on the silicon wafers causes substantial changes of the surface morphology (Fig. 1b) and a PSD spectrum (Fig. 2). The top surface of the Al/Zr multilayer consists of numerous hillocks and troughs of different

sizes randomly distributed over the surface. The smallest surface features observed are about of 0.1 nm high and have an apparent lateral size of about 10 nm, which corresponds to the AFM tip radius of 7 nm. The middle frequency component of surface roughness increases by an order of magnitude as compared to the silicon substrate. As a result of this, a knee in the white noise roughening is apparent on the PSD curve at the frequency of 0.01 nm^{-1} . The net roughness measured over a $1 \times 1 \mu\text{m}^2$ area increases to $\sim 0.27 \text{ nm rms}$.

The slope of the PSD at the right from the knee indicates a smoothing of the high-frequency ($f \geq 0.01 \text{ nm}^{-1}$) component of the white noise. Theoretical PSD functions shown with solid curves in Fig. 2 were calculated with the linear model (equations 2, 4, and 5) for the different smoothing mechanisms. We assumed that the roughness at low frequencies ($f \approx 0.001 \text{ nm}^{-1}$ and less) comes from the substrate with a PSD modeled as a power law $\text{PSD} \sim 1/f^{1.9}$. The parameters of the calculated PSDs are listed in the Table 1. Since the exponent $n=4$ provides the best fit to the experimental data, one can conclude that surface diffusion is the main mechanism of surface relaxation for the Al/Zr multilayers.

An increase in the total thickness of an Al/Zr multilayer up 1040 nm by deposition of a larger number of the bi-layers ($N=104$) of the same thickness results in further roughening of the surface (Fig. 1b). The PSD spectrum demonstrates growth of a white noise level and a shift of the knee towards lower frequencies. Observed changes of the roughness and the PSD are in completely consistent with the model predictions (red solid and blue dash curves in Fig. 2). Both of the experimental PSD are fitted with the same fitting parameters $n=4$, $\Omega=7 \text{ nm}^3$, and $\nu=120 \text{ nm}^3$, for the two coating thicknesses (Table 1).

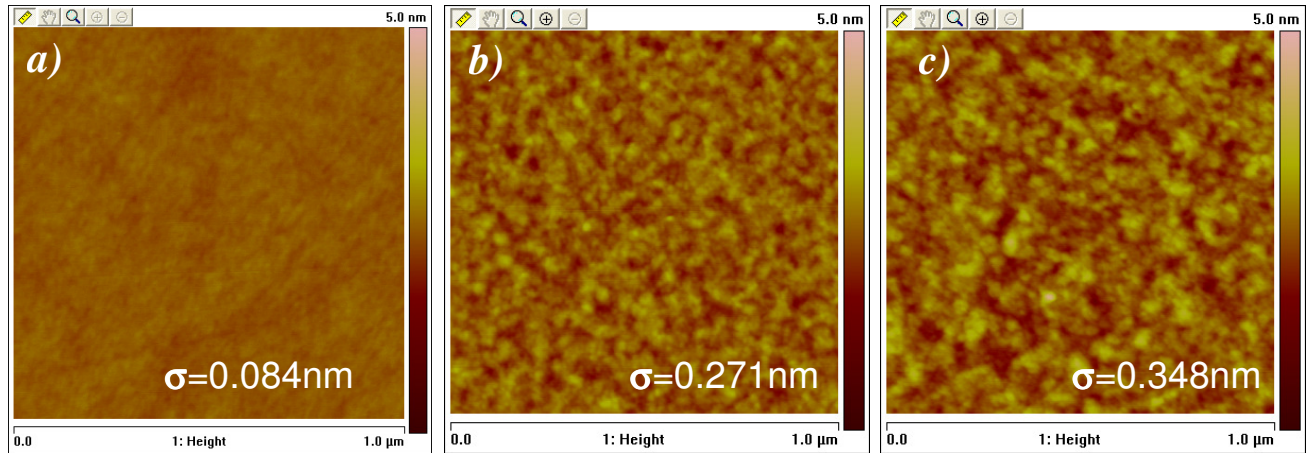


Figure 1. AFM images of a surface of a silicon wafer (a) and top surface of Al/Zr multilayers (b,c) deposited on the wafer. The multilayers consist of 20 Al-Zr bi-layers with total thickness of 200 nm (b) and 104 bi-layers with the thickness of 1040 nm (c).

The model PSD curves deviate from the experimental data at the frequencies higher than $f \approx 0.03 \text{ nm}^{-1}$ and demonstrate a higher slope than the exponent $n=4$ predicts. Such a deviation was observed by C. Eisenmenger-Sittner for very thin Al films [13]. The PSD slope was fitted with $n \approx 5$ for very thin films and reduced gradually to $n=4$ as thickness of the film increased. The author concluded that high initial slope should be attributed to an island stage of a film growth, when a surface height distribution and hence PSD functions are described by a Gaussian function rather than a power law. This approach seems to be very reasonable with regard to growth of Al/Zr multilayer composed of very thin layers. Though the layers are continuous, their surface morphology still inherits its island growth prehistory. Further improvement of the linear model by incorporation island growth kinetics is necessary to provide more adequate PSD simulations.

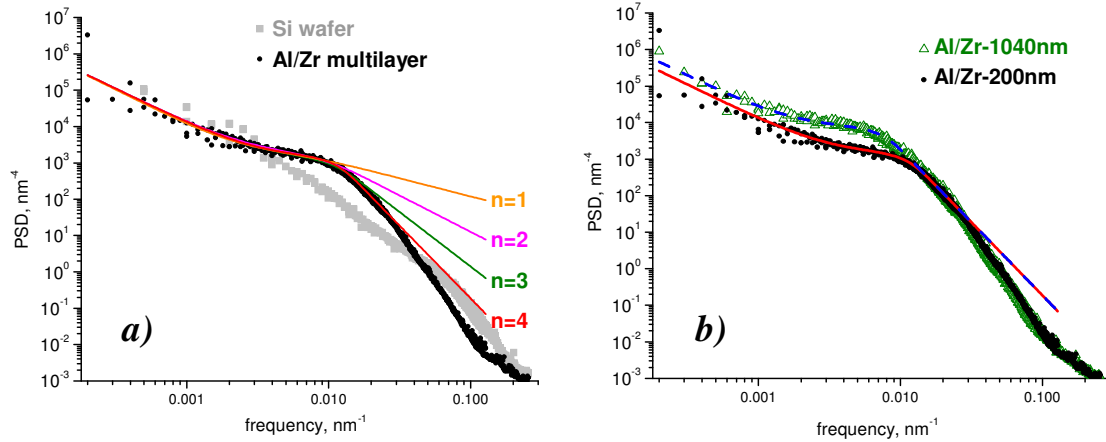


Figure 2. (a) PSD spectra for a surface of a flat silicon substrate (grey squares) and top surface of Al/Zr-20 multilayer (black circles) deposited on the substrate. Solid lines show fits of the multilayer PSD with the formula (2, 4) for different values of the frequency exponent. (b) PSD spectra for Al/Zr multilayers with total thickness of 200 nm (black circles) and 1040 nm (green triangles). Solid and dash curves show calculated PSD functions for fitting parameters $n=4$, $\Omega=7 \text{ nm}^3$, and $v=120 \text{ nm}^3$.

Table 1. Parameters of the PSD functions (shown in Fig. 2a) of the top surface of the Al/Zr multilayers deposited on a flat substrates, calculated for different values of the exponent, n .

n	$\Omega, \text{ nm}^3$	v_n	$l, \text{ nm}$	$d, \text{ nm}$
1	15	0.1 (unitless)	-	200
2	10	1 (nm)	1	200
3	7	10 (nm^2)	3.2	200
4	7	120 (nm^3)	5	200
4	7	120 (nm^3)	5	1040

An AFM image of a saw-tooth substrate with the period of 100 nm is shown in Fig. 3a, and a correspondent PSD function is shown in Fig. 4 with a grey curve. Since the surface is highly anisotropic, a one dimensional PSD function is shown, which differs from a two dimensional one only by a frequency normalization, and also can be used for the smoothing analysis.

Due to the high asymmetry of the saw-tooth groove profile, the PSD spectrum of the substrate exhibits a number of peaks corresponding the main surface frequency of 0.01 nm^{-1} and multiple harmonics. Deposition of the Al/Zr multilayers on the saw-tooth substrate results in significant smoothing of the grooves and suppression of the harmonics. Initially triangular grooves transforms to almost sinusoidal shape (Fig. 3b). PSD spectrum for the MBG surface shows however that the second Fourier harmonics of the surface still survives (an orange curve in Fig. 4). It indicates the groove profile is not an ideal sine function but still keeps some asymmetry.

The smoothing process was modeled with the Equation (4), i. e. the substrate PSD was multiplied by a replication factor squared, and added to the film PSD, and then compared with the top surface PSD. In order to generate the film PSD an additional AFM image of the coated grating was taken similarly to the one in Fig. 3b, but by scanning along the grooves. Then the image was flattened by subtracting a DC component (i. e. an average height) of height for each line of the scan.

This procedure removes a sine-like component of the surface relief, leaving only a stochastic roughness component. A one dimensional PSD function (a cyan curve in Fig. 4) obtained from the flattened image is almost identical to the one for the flat multilayer (not shown) at frequencies of 0.01 nm^{-1} and higher, where the surface topography is defined by intrinsic roughness of the multilayer. At lower frequencies, where replication dominates smoothing, some minor difference is caused by the difference of the surface roughness for flat and saw-tooth substrates..

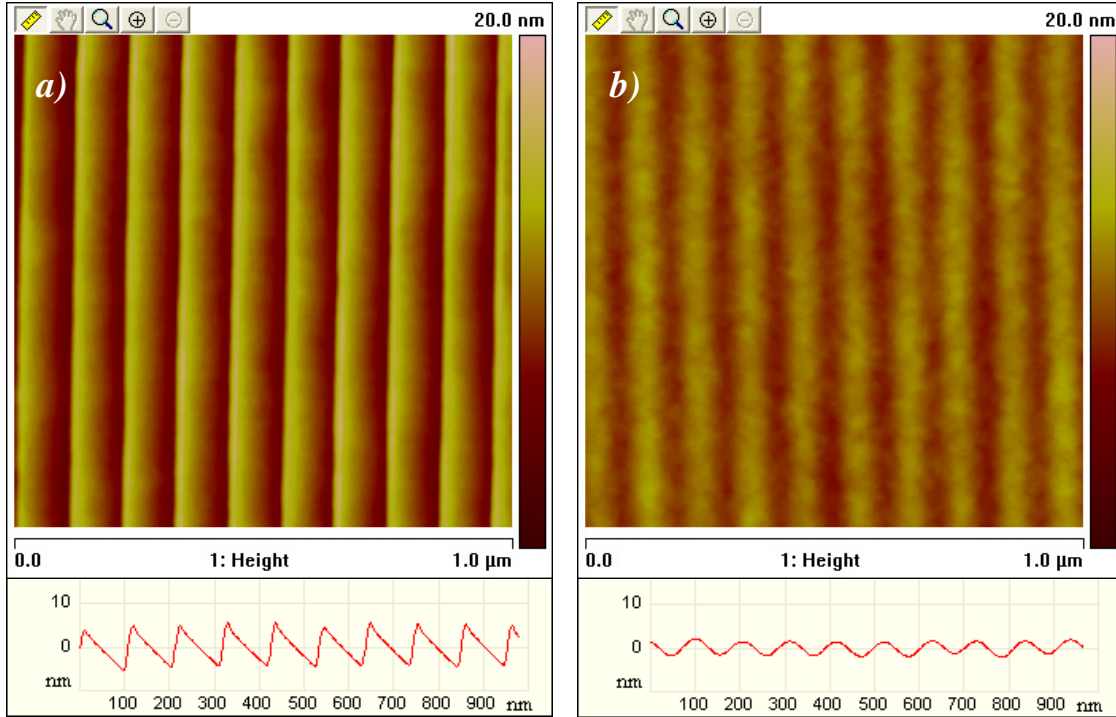


Figure 3. AFM images and average profiles of a surface of a saw-tooth substrate before Al/Zr multilayer deposition (a) and the top surface of the ML-coated grating (b).

Parameters of the replication factors for different smoothing mechanisms are listed in Table 2. The parameters were fitted to provide an experimentally observed fivefold suppression of the 1st saw-tooth harmonic with the frequency of $f=0.01 \text{ nm}^{-1}$. The frequency dependence of the factors with the exponents $n=1, 2, 3,$ and 4 are shown in the left bottom part of the plot with black, blue, green, and red curves and circles respectively. The same colors were used for PSD functions modeled for respective smoothing mechanisms.

It turns out that smoothing parameters $n=4$ and $v_4=120 \text{ nm}^3$ obtained for the flat multilayer (Table 1) do not provide a fivefold suppression of the 1st PSD peak, but only twofold one (not shown). To fit the intensity of the 1st peak one needs to increase the relaxation parameter by more than a factor of 2 (Table 2). The replication factor and PSD function modeled with $n=4$ and $v_4=250 \text{ nm}^3$ are shown with the red line and open circles in Fig. 4.

Comparison of the modeled PSD function to the experimental one shows that the exponent $n=4$ causes too strong suppression of high frequencies. The 2nd PSD peak with the frequency of $f=0.02 \text{ nm}^{-1}$ vanishes completely since its intensity is far below the level of intrinsic roughness of the multilayer. The PSD function modeled with the exponent $n=3$ demonstrates the same behavior (see blue curves in Fig. 4). On the other hand the exponent $n=1$ does not provide enough suppression of the 2nd, 3rd, 4th, and even 5th high frequency harmonics. Only a PSD function with the exponent $n=2$ is in reasonable consistency with the experimentally observed PSD.

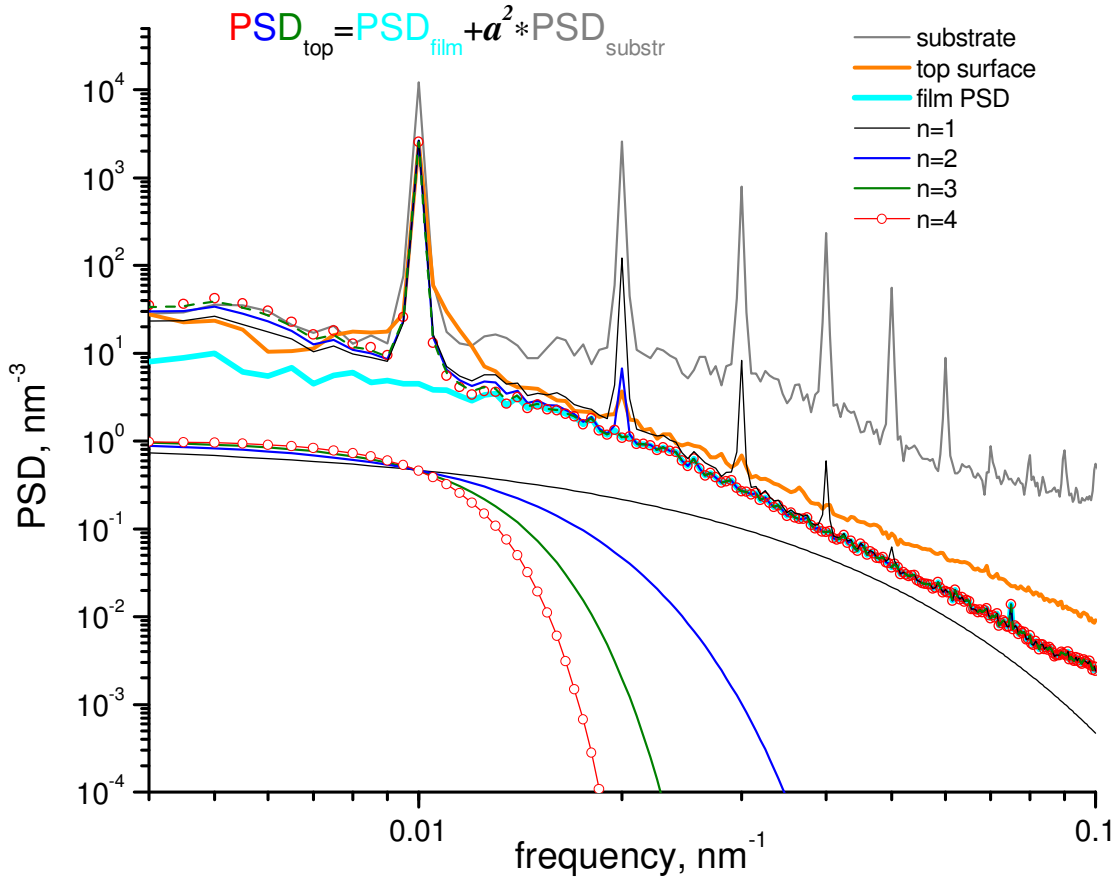


Figure 4. One-dimensional PSD spectra for the saw-tooth substrate before (a grey curve) and after (an orange curve) deposition of the Al/Zr multilayer. The film PSD spectrum (see comments in the text) is shown with a cyan curve. PSD functions of the ML-coated grating calculated with the formula () for the different smoothing mechanisms are shown with black (n=1), blue (n=2), olive (n=3) curves and red open circles (n=4). The black, blue, olive curves and open circles in the bottom part of the plot show corresponding replication factors used for the simulations.

Table 2. Parameters of the PSD functions (shown in Fig. 4) of the top surface of the Al/Zr multilayer coated saw-tooth substrate, calculated for different values of the exponent, n.

n	v_n	l , nm	d , nm
1	0.061 (unitless)	-	200
2	0.97 (nm)	0.97	200
3	15.7 (nm ²)	3.96	200
4	250 (nm ³)	6.3	200

4. DISCUSSION

Results obtained show that smoothing of the surface features with Al/Zr multilayers occurs in different ways for flat and saw-tooth substrates. The linear model shows that surface diffusion with exponent $n=4$ is a main relaxation mechanism for flat multilayers. However, growth parameters found for flat multilayers cannot explain the decay of PSD peaks during deposition on a saw-tooth substrate. Smoothing of saw-tooth substrates occurs via some other kinetics with effective exponent $n=2$. This discrepancy in multilayer growth behavior for different substrates is dissimilar to the smoothing of surface features with Mo/Si multilayers observed by Stearns et al. [12]. The authors used the same set of fitting parameters to simulate Mo/Si growth on flat substrates and substrates with artificial surface defects having a high aspect ratio. Note however, the multilayers were deposited with ion-beam sputtering which is quite different technique as compared to dc-magnetron sputtering used in present work in terms of the energy of the sputtered atoms and smoothing mechanisms. The dominating mechanism was found to be described predominantly with the exponent $n=2$ for both kinds of substrates. (The authors considered also smoothing with the exponent $n=4$, a contribution of the surface diffusion in the smoothing is by 10-1000 times smaller as compared to smoothing with the exponent $n=2$ for the frequency range of 0.1-0.01 nm^{-1} . The ratio of contribution can be estimated as $v_4 f^4 / v_2 f^2$.)

The discrepancy of theoretical and experimental smoothing behavior was observed by Roder et al. for successive smoothing of substrates having a rippled surface with ZrO_2 amorphous coatings in the course of pulsed laser deposition [14]. The authors noticed that high frequency harmonics of PSD spectra decay much slower than the model predicted. They concluded that the model was not complex enough, and assumed that relaxation parameters, v_n , could depend on film thickness. Such an assumption seems quite reasonable for the monolayer coatings, especially for polycrystalline ones such as Al or Zr, since a complicated evolution of grain shape and size occurs with the coating thickness [13]. However, we would not expect some dependence of relaxation parameters on ML thickness. Each layer grows via a complicated processes of nucleation, island growth and coalescence, and surface smoothing. The processes determine the structure and surface morphology of individual layers, which depend on layer thickness. However, all the Al (Zr) layers have the same thickness, and increase of ML thickness by adding new layers does not affect the structure of individual layer, grain size etc.

In our opinion the reasons for the different growth behavior could come from the different geometry of the deposition caused by the different shape of the substrates. The surface of a multilayer growing on a flat substrate has local slope variations caused by an intrinsic roughness of the coating. The variations are relatively small, which is why the linear model provides adequate description of the surface morphology for a number of coatings including multilayers [6]. Even for Al/Zr multilayer composed of crystalline materials, the model provides precise prediction of PSD evolution with the multilayer thickness (Fig. 2).

In contrast to flat wafers a saw-tooth substrate has highly tilted facets. This modifies the deposition geometry and can trigger an additional component of surface mass transfer, as illustrated in Fig. 5. During a deposition an average atomic flux is uniform, but tilted surfaces receive a lower amount of a material according to the cosine law, and therefore the concentration of adatoms is smaller for highly tilted areas. A gradient of concentration of the adatoms results in additional surface diffusion flux which provides a mass transfer from less tilted areas to highly tilted ones as schematically shown with solid arrows in Fig. 5.

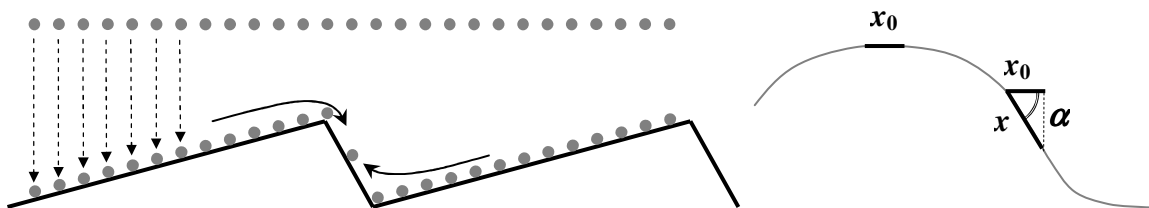


Figure 5. Deposition geometry for a saw-tooth substrate is sketched schematically. Concentration of adatoms (grey circles) depends on a local tilt of the surface. A gradient of concentration of the adatoms results in diffusion fluxes, depicted by arrays, from less tilted areas towards highly tilted ones.

When N atoms land in a horizontal area, x_0 , of a surface $h(x,t)$, concentration of adatoms is $C_0 = N / x_0$. For a surface tilted by an angle α the same amount of atoms is distributed over larger area, x ,

$$x = \sqrt{x_0^2 + (x_0 \tan \alpha)^2} = x_0 \sqrt{1 + (\nabla h)^2} \quad (6)$$

Then the concentration of adatoms is:

$$C = C_0 (1 + (\nabla h)^2)^{-\frac{1}{2}} \approx C_0 - \frac{C_0}{2} (\nabla h)^2 \quad (7)$$

and the concentration gradient is

$$\nabla C = -\frac{C_0}{2} \nabla (\nabla h)^2 \quad (8)$$

and will result in a diffusion flux

$$j = -D \nabla C \sim \nabla (\nabla h)^2 \quad (9)$$

where D is a surface diffusion coefficient.

Then time (or thickness) evolution of the surface caused by an adatom concentration gradient is

$$\left(\frac{\partial h}{\partial t} \right)_\alpha = -\text{div} j \sim -\nabla^2 (\nabla h)^2 \quad (10)$$

This nonlinear term should be added into the linear equation (1) of the growth. Then full growth equation is

$$\frac{\partial h}{\partial t} = -v_n \nabla^n h - \lambda \nabla^2 (\nabla h)^2 + \eta \quad (11)$$

This equation was proposed by J. Willian [15] and was considered originally for molecular beam epitaxial growth by Z.W.Lai and S. Das Sarma [16], but with a positive sign before the non-linear term. It is interesting to consider smoothing of a sine profile by surface diffusion. In this case the first term describes mass transfer from peaks to valleys and results in a gradual decay of the sine amplitude. The second term describes diffusion from both peaks and valleys towards slopes. This process causes reduction of the peak height and at the same time deepening of the valleys, so the resulting amplitude of the surface profile does not changes significantly. The degradation of the initial sine profile occurs not via amplitude decay as for the first term, but via widening of peaks and narrowing of valleys (see an insertion in Fig. 6). Valleys trend to collapse and transform in narrow spikes (but they will be partially smoothed by the first linear term.) Such surface evolution means growth of high frequency harmonics in a surface Fourier spectrum and PSD function. Hence, the nonlinear term withstands the suppression of the high-frequency PSD peaks with surface diffusion driven by a gradient of chemical potential caused by surface curvature (the linear term).

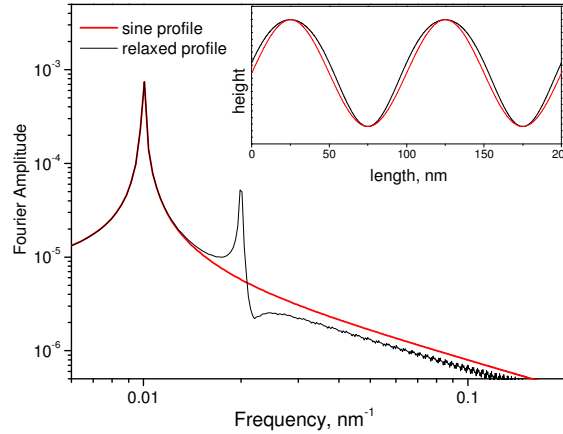


Figure 6. Illustration of the impact of the non-linear relaxation term (see eq. 10) on a profile and a Fourier spectrum of an initially sinusoidal surface.

Although we found that a replication factor with the exponent $n=2$ provides a good agreement of the observed PSD decay (Fig. 4) its physical meaning is not well clear. It should be considered as some effective parameter rather than a one which can be attributed to some smoothing mechanism. Note, it is not possible to simulate the PSD decay assuming both $n=2$ and $n=4$ process presenting during the smoothing of the saw-tooth substrate. In other words the linear model fits in Fig. 4 show not only that a process with $n=2$ was switched on for the saw-tooth substrate, but also the surface diffusion smoothing process with $n=4$ was switched off, which is difficult to explain. Detailed analysis of evolution of a profile of saw-tooth substrates during multilayer deposition using the nonlinear model (Equation (11)) should be performed. This work is currently in progress.

5. CONCLUSIONS

A linear continuum model provides a reasonable modeling of PSD spectra of Al/Zr multilayers grown on a flat substrate. Some discrepancy at high frequencies can be attributed to the processes of nucleation, island growth and coalescence, which are not considered in the framework of the model. Nevertheless the model provides correct prediction for the thickness evolution of the PSD spectra. It was found that surface diffusion described with the relaxation exponent $n=4$ is the main relaxation mechanism for flat multilayers in this case

However, the linear model is unable to describe the growth of the same multilayer on flat and saw-tooth substrates with the same set of relaxation parameters. The model yields an effective smoothing exponent $n=2$ for the observed decay of the PSD of saw-tooth substrates during deposition. Such a discrepancy indicates that growth of the multilayer on a saw-tooth substrate occurs in a quite different manner as compared to the one for a flat substrate. This is a result of limitations in the linear model which assumes only slight variations of the local surface slope, while a saw-tooth substrate has highly tilted facets. A simple geometrical analysis of the deposition geometry for a saw-tooth substrate indicates that a non-linear term, $-\lambda \nabla^2 (\nabla h)^2$, should be added to the growth equation to adequately describe the smoothing process.

ACKNOWLEDGEMENTS

The Advanced Light Source is supported by the Director, Office of Science, Office of Basic Energy Sciences, Material Science Division, of the U.S. Department of Energy under Contract No. DE-AC02-05CH11231 at Lawrence Berkeley National Laboratory.

DISCLAIMER

This document was prepared as an account of work sponsored by the United States Government. While this document is believed to contain correct information, neither the United States Government nor any agency thereof, nor The Regents of the University of California, nor any of their employees, makes any warranty, express or implied, or assumes any legal responsibility for the accuracy, completeness, or usefulness of any information, apparatus, product, or process disclosed, or represents that its use would not infringe privately owned rights. Reference herein to any specific commercial product, process, or service by its trade name, trademark, manufacturer, or otherwise, does not necessarily constitute or imply its endorsement, recommendation, or favoring by the United States Government or any agency thereof, or The Regents of the University of California. The views and opinions of authors expressed herein do not necessarily state or reflect those of the United States Government or any agency thereof or The Regents of the University of California.

REFERENCES

- [1] D.L. Voronov, M. Ahn, E.H. Anderson, R. Cambie, Ch.-H. Chang, E.M. Gullikson, R.K. Heilmann, F. Salmassi, M.L. Schattenburg, T. Warwick, V.V. Yashchuk, L. Zipp, H.A. Padmore, "High-efficiency 5000 lines/mm multilayer-coated blazed grating for extreme ultraviolet wavelengths," *Opt. Lett.* **35**, 2615-2618 (2010).
- [2] A. Kotani, Sh. Shin, "Resonant inelastic x-ray scattering spectra for electrons in solids," *Rev. Mod. Phys.* **73**, 203-246 (2001).
- [3] D.L. Voronov, M. Ahn, E.H. Anderson, R. Cambie, Ch.-H. Chang, L.I. Goray, E.M. Gullikson, R.K. Heilmann, F. Salmassi, M.L. Schattenburg, T. Warwick, V.V. Yashchuk, and H.A. Padmore, "High efficiency multilayer blazed gratings for EUV and soft X-rays: Recent developments," *Proc. SPIE* **7802**, 780207-1 - 780207-13 (2010).
- [4] D.L. Voronov, E.H. Anderson, R. Cambie, S. Cabrini, S.D. Dhuey, L.I. Goray, E.M. Gullikson, F. Salmassi, T. Warwick, V.V. Yashchuk, and H.A. Padmore, "A 10,000 groove/mm multilayer coated grating for EUV spectroscopy," *Opt. Express* **19** (7), 6320-6325 (2011).
- [5] W. M. Tong and R. S. Williams, "Kinetics of surface growth: phenomenology, scaling, and mechanisms of smoothing and roughening," *Annu. Rev. Phys. Chem.* **45**, 401-438. (1994).
- [6] C. Herring, "Effect of change of scale on sintering phenomena," *J. Appl. Phys.* **21**, 301-303 (1950).
- [7] M. Moseler, P. Gumbsch, C. Casiraghi, A. C. Ferrari, and J. Robertson, "The Ultrasmoothness of Diamond-like Carbon Surfaces," *Science* **309**, 1545-1548 (2005).
- [8] R. Mark Bradley James M. E. Harper, "Theory of ripple topography induced by ion bombardment," *J. Vac. Sci. Technol. A* **6** (4), 2390-2395 (1988).
- [9] E. Spiller, S. Baker, E. Parra, C. Tarrío, "Smoothing of Mirror Substrates by Thin-Film Deposition," *Proc. SPIE* **3767**, 143-153 (1999).
- [10] D.G. Stearns, D.P. Gaines, D.W. Sweeney, E.M. Gullikson, "Nonspecular x-ray scattering in a multilayer-coated imaging system," *J. Appl. Phys.* **84**, 1003-1028 (1998).
- [11] D.G. Stearns, P.B. Mirkarimi, E. Spiller, "Localized defects in multilayer coatings," *Thin Solid Films* **446**, (2004) 37-49.
- [12] P. Philippe, S. Valette, O. Mata Mendez, D. Maystre, "Wavelength demultiplexer: using echelette gratings on silicon substrate," *Appl. Opt.* **24**, 1006-1011 (1985).
- [13] C. Eisenmenger-Sittner, "Surface evolution of polycrystalline Al films deposited on amorphous substrates at elevated temperatures," *J. Appl. Phys.* **89**, 6085-6091 (2001).
- [14] H. Roder, H.-U. Krebs, "Frequency dependent smoothing of rough surfaces by laser deposition of ZrO₂," *Appl. Phys. A* **90**, 609-613 (2008).
- [15] J. Villain, "Continuum models of crystal growth from atomic beams with and without desorption," *J. Phys. C*, **11**, 19-42 (1991).
- [16] Z.-W. Lai and S. Das Sarma, "Kinetic Growth with Surface Relaxation: Continuum versus Atomistic Models," *Phys. Rev. Lett.* **66**, 2348-2351 (1991).